

Lawrence Berkeley National Laboratory

Lawrence Berkeley National Laboratory

Title

The DEEP2 Galaxy Redshift Survey: AEGIS observations of a Dual AGN at $z = 0.7$

Permalink

<https://escholarship.org/uc/item/3jb4v7kc>

Authors

Gerke1, Brian F.
Newman, Jeffrey A.
Lotz, Jennifer
et al.

Publication Date

2006-10-13

Peer reviewed

The DEEP2 Galaxy Redshift Survey: AEGIS observations of a Dual AGN at $z = 0.7$

Brian F. Gerke¹, Jeffrey A. Newman^{2,3}, Jennifer Lotz⁴, Renbin Yan⁵, P. Barmby⁶, Alison L. Coil^{2,7}, Christopher J. Conselice⁸, R. J. Ivison^{9,10}, Lihwai Lin¹¹, David C. Koo¹², Kirpal Nandra¹³, Samir Salim¹⁴, Todd Small¹⁵, Benjamin J. Weiner¹⁶, Michael C. Cooper⁵, Marc Davis^{1,5}, S. M. Faber¹², Puragra Guhathakurta¹²

bgerke@astro.berkeley.edu

ABSTRACT

We present evidence for a dual Active Galactic Nucleus (AGN) within an early-type galaxy at $z = 0.709$ in the Extended Groth Strip. The galaxy lies on the red sequence, with absolute magnitude $M_B = -21.0$ (AB, with $h = 0.7$) and rest-frame color $U - B = 1.38$. Its optical spectrum shows strong, double-peaked [O III] emission lines and weak $H\beta$ emission, with Seyfert-like line ratios. The two

¹Dept. of Physics, U.C. Berkeley, Berkeley, CA 94720, bgerke@berkeley.edu

²Hubble Fellow

³Lawrence Berkeley National Laboratory, Berkeley, CA 94720

⁴Leo Goldberg Fellow, NOAO, Tucson, AZ 85719

⁵Dept. of Astronomy, U.C. Berkeley, Berkeley, CA 94720

⁶Harvard-Smithsonian Center for Astrophysics, Cambridge, MA 02138

⁷Steward Observatory, U. of Arizona, Tucson, AZ 85721

⁸School of Physics and Astronomy, U. of Nottingham, University Park NG9 2RD UK

⁹UK Astronomy Technology Centre, Royal Observatory, Blackford Hill, Edinburgh EH9 3HJ, UK

¹⁰Institute for Astronomy, U. of Edinburgh, Blackford Hill, Edinburgh EH9 3HJ, UK

¹¹Dept. of Physics, National Taiwan University, Taiwan

¹²UCO/Lick Observatory, UCSC, Santa Cruz, CA 95064

¹³Astrophysics Group, Imperial College, London SW7 2BZ UK

¹⁴Dept. of Physics and Astronomy, UCLA, Los Angeles, CA 90095

¹⁵Space Astrophysics, 405-47, Caltech, Pasadena, CA 91125

¹⁶Dept. of Astronomy, U. of Maryland, College Park, MD 20742

narrow peaks are separated by 630 km s^{-1} in velocity and arise from two distinct regions, spatially resolved in the DEIMOS spectrum, with a projected physical separation of 1.2 kpc. *HST*/ACS imaging shows an early-type (E/S0) galaxy with hints of disturbed structure, consistent with the remnant of a dissipationless merger. Multiwavelength photometric information from the AEGIS consortium confirms the identification of a dust-obscured AGN in an early-type galaxy, with detections in X-ray, optical, infrared and radio wavebands. These data are most readily explained as a single galaxy harboring two AGN—the first such system to be observed in an otherwise typical early-type galaxy.

Subject headings: galaxies:active — galaxies:nuclei

1. Introduction

The standard picture of AGN emission—which identifies the engines as accreting supermassive black holes (SMBHs)—is now well established. Also well established is the hierarchical paradigm for structure formation, in which massive galaxies grow via a series of mergers of smaller objects. An obvious consequence of this picture is that some galaxies should contain two SMBHs in their centers. Such nuclear BH pairs will initially be widely separated ($\gtrsim 1 \text{ kpc}$) “dual” SMBHs. After $\sim 100 \text{ Myr}$ they will become true *binary* SMBHs, gravitationally bound to one another and with parsec-scale separations; they may finally coalesce into a single central SMBH on much longer timescales (Begelman, Blandford, & Rees 1980). The behavior of SMBH binaries has significant implications for the formation of galactic cores (e.g., Milosavljević et al. 2002), and their coalescence may be a significant source of gravitational radiation in the universe; this subject has received much theoretical study (for a review see Merritt & Milosavljević 2005).

Observational study of these objects has been far more limited, however: only recently has direct detection of a true binary SMBH been reported, in the LINER-like elliptical radio galaxy 0402+379 (Maness et al. 2004; Rodriguez et al. 2006). In addition, there is only one unambiguous detection of a dual AGN in a single galaxy, from *Chandra* studies of the merger remnant NGC 6240 (Komossa et al. 2003), although there are several examples of merging pairs of AGN hosts (e.g., Ballo et al. 2004; Guainazzi et al. 2005; Hudson et al. 2006), and there is a population of close quasar pairs that are very unlikely to be lensed objects (e.g. Kochanek, Falco & Muñoz 1999; Junkkarinen et al. 2001). Most of the merger examples were discovered in studies of merging late-type galaxies with significantly disturbed morphologies. Recent work on galaxy evolution (e.g., Faber et al. 2005) implies that significant stellar mass in elliptical galaxies is built up in dissipationless mergers of early-type progenitors. The

remnants of such mergers exhibit only subtle visual signatures (van Dokkum et al. 2005), suggesting that dual-SMBH systems should also occur in apparently normal early-types.

The Extended Groth Strip is a subregion of the DEEP2 Galaxy redshift survey that is also the site of intense, multiwavelength observational efforts by the All-wavelength Extended Groth strip International Survey (AEGIS) team. Full details of the dataset can be found in Davis et al. (2006). In this Letter, we present evidence from AEGIS for a dual AGN at $z = 0.709$ in the $R_{AB} = 22.6$ early-type galaxy EGSD2 J142033.66+525917.5. The object was identified serendipitously in the process of visually inspecting DEEP2 spectra to confirm galaxy redshifts. Throughout this work we adopt a flat, Λ CDM cosmology with $\Omega_M = 0.3$ and $h = 0.7$; all distances are quoted in physical (not comoving) units.

2. Observations

Fig. 1 shows part of the one-dimensional DEEP2 spectrum of this object, obtained using the DEIMOS spectrograph on the Keck II telescope. The most notable features of the spectrum are a pair of strong, double-peaked emission lines, readily identifiable by their wavelength ratios as [O III] $\lambda 4959$ and $\lambda 5007$. The two peaks of the $\lambda 5007$ line are separated by 17.8\AA in wavelength. The spectrum also has $H\beta$ emission, which may be double-peaked but is partially obscured by residual night-sky Poisson noise; there are no other emission lines, but the spectrum displays a numerous stellar continuum absorption features over the entire observed wavelength range ($6750\text{--}8890\text{\AA}$), most of which is not shown here. Fig. 2 shows the sky-subtracted two-dimensional DEIMOS spectrum of this object in the regions around each of the emission lines seen in Fig. 1. The spectrum exhibits two *spatially offset* emission components: their spatial centroids (which can be measured independently to an accuracy of ~ 0.1 pixels) are separated by 1.5 DEIMOS pixels, or $0''.17$ on the sky. The two components have spatial extents that are consistent with the $\sim 0''.6$ seeing on the night of observation; they are not extended sources.

Because the emission lines in this spectrum have significant velocity structure, we determined the systemic redshift of the galaxy by fitting synthetic spectral templates to the galaxy’s stellar continuum emission, whose absorption features do not exhibit such structure. Following Yan et al. (2006), we use the stellar population synthesis code of Bruzual & Charlot (2003) to create two templates, representing an old (7 Gyr) population and a young (0.3 Gyr) population, both with solar metallicity. We then find the redshift and the linear combination of these templates that best fit the observed spectrum, excluding wide windows around the $H\beta$ and [O III] lines. Only the old-population template proved necessary for a good fit. This procedure yields a redshift of $z = 0.709$ for the host galaxy. The K-correction

algorithm of Willmer et al. (2005) then gives an absolute magnitude $M_B = -21.0$ (AB) and a rest-frame color $U - B = 1.38$ —among the reddest in DEEP2, though typical of AGN (Nandra et al. 2006). We have shifted the wavelength scale of Fig. 1 to the rest frame of the host; the expected wavelengths of the emission lines are shown by vertical dashed lines. The two emission peaks are located almost symmetrically with respect to the host galaxy in velocity space. In the host’s rest frame, their velocity separation is 630 km s^{-1} and their projected physical separation is 1.2 kpc.

Having fit the stellar continuum, we may subtract off this emission and consider the properties of the emission lines alone. First, the two emission-line components have strongly asymmetric profiles. The emission lines seen in Fig. 1 are not well described by the sum of two Gaussian curves; there is significant emission bridging the two peaks. We therefore fit the spectrum with *three* Gaussians by iteratively fitting and subtracting first the blueward peak, then the redward, then the bridging emission. This yields velocity dispersion measurements of $54 \pm 2 \text{ km s}^{-1}$ and $95 \pm 4 \text{ km s}^{-1}$ for the blueward and redward emission components, respectively. The bridging emission is too uniformly distributed in wavelength to be particularly well described a Gaussian, but its nominal dispersion is $150 \pm 8 \text{ km s}^{-1}$, and its peak is consistent with zero velocity offset. The ratio of the [O III] $\lambda 5007$ and $H\beta$ line fluxes is commonly used to distinguish Seyfert galaxies from other emission-line galaxies, with Seyferts having $\lambda 5007/H\beta > 3$ in the local universe (e.g., Kauffman 2003); this criterion remains valid for red galaxies at $z \sim 1$ (R. Yan et al. in prep.). We have measured the ratios for the two emission components in this red galaxy by summing the 1-d spectrum over the measured 1σ velocity width of each peak. This procedure gives ratios of 11.9 ± 0.4 and 15.8 ± 0.4 for the blueward and redward component, respectively, placing both firmly in the Seyfert category.

We now turn to multiwavelength imaging from the AEGIS collaboration. Of the available imaging data, only the *HST*/ACS images have the potential to resolve the two emission regions; we show ACS imaging in the F606W and F814W (hereafter *V* and *I*) bands in Fig. 3. Also shown are the positions of the DEIMOS slit edges and the positions along the slit of the emission components seen in Fig. 2. The *I* band image shows an early-type, spheroidal galaxy with a smooth profile, but the image also exhibits subtle asymmetry, with a nucleus that is slightly off-center compared to the outer envelope; this may indicate recent merger activity. The *V* band image is less smooth and more obviously asymmetric. It also shows an interesting horseshoe-shaped structure near its center on a similar angular scale as the galaxy’s two emission-line components; this structure might be related to the emission regions.

We have run the GALFIT galaxy image modeling code (Peng et al. 2002) on the ACS

images, and we find that both radial profiles are described well by a Sérsic (1968) profile, with index $n=2.14$ for the I band and $n=1.7$ for the V band. The images' central concentrations are thus near the low end of the elliptical range. Also, the morphological parameters computed by Lotz et al. (2006) for the ACS imaging are consistent with expectations for bulge-dominated galaxies, but with a significantly lower concentration and higher degree of substructure than are typical for such objects. These results support the picture of an early-type galaxy with a double nucleus.

In Fig. 4, we compile a rest-frame SED from AEGIS observations. The object is detected at $> 3\sigma$ significance in *Chandra*/ACIS imaging, ground-based *BRIK* photometry from CFHT and Palomar, all four *Spitzer* IRAC bands, the *Spitzer* MIPS 24 μm band, and at 21cm with the VLA. We also show 3σ upper limits on the flux in the *GALEX* bands and at 6cm.

The measured SED is well described by the simple model of an early-type galaxy with a central, dust-obscured AGN. Plotted in Fig. 4 is a synthetic SED, produced using the code of Bruzual & Charlot (2003), representing a galaxy with an old (7 Gyr), dust-free stellar population that formed in a single 500 Myr burst; it has been normalized to the measured K band flux of the host galaxy, and no further fitting has been done in the figure. To obtain more precision, we have applied the SED template-fitting procedure of Salim et al. (2005) to the *BRIK* fluxes alone: this galaxy has a 7-Gyr-old stellar population with a stellar metallicity 1.1 ± 0.2 times solar, a stellar mass of $\log(M_*/M_\odot) = 11.00 \pm 0.07$, a star formation rate of $\log[(\dot{M}_*/(1M_\odot\text{yr}^{-1}))] = -0.97 \pm 0.35$ and a V band dust extinction of 0.30 ± 0.14 mag. Also plotted in the Figure is a simple model of the emission from a dust-obscured AGN, normalized to the 24 μm flux, to illustrate that dust can account for the MIPS flux without contributing significant emission at shorter wavelengths. The curve was produced using the publicly available DUSTY code for radiative transfer through dust (Ivezic, Nenkova, & Elitzur 1999), with a simple hot-dust model after Gandhi et al. (2001), and an input spectrum given by the mean SED for radio-loud quasars (Elvis et al. 1994). The *Chandra* observation is also consistent with an obscured AGN: of nine photons detected from this source seven are in the hard (2–7 keV) X-ray band, indicating that the soft (0.5–2 keV) X-ray emission has been absorbed. Assuming an intrinsic X-ray spectrum $F_\nu \propto \nu^{-0.9}$, the X-ray data imply an absorption-corrected X-ray luminosity of 1.7×10^{42} erg s $^{-1}$ in the rest-frame 2–10 keV band. Similarly, assuming a radio spectrum $F_\nu \propto \nu^{-0.8}$, the 21 cm emission translates into a rest-frame 1.4 GHz luminosity of $(1.8 \pm 0.6) \times 10^{23}$ erg s $^{-1}$ Hz $^{-1}$ (see Ivison et al. 2006 for details).

3. Discussion

These observations represent strong evidence for a dual AGN hosted by an early-type galaxy. The [O III] $\lambda 5007/H\beta$ emission-line ratio of the galaxy is iron-clad evidence for an AGN; this is further supported by the X-ray detection. The conclusion that there are in fact *two* accreting SMBHs in this galaxy is driven entirely by the DEEP2 spectroscopic data. Double peaked emission lines like those seen in Fig. 1 could be explained by three reasonable models: a rotating disk, an outflow (or inflow), or a pair of orbiting emission components. A reasonable disk model, however, cannot easily accommodate emission regions separated by 1.2 kpc and 630 km s^{-1} . Typical accretion disks around SMBHs are smaller by several orders of magnitude and have relativistic velocities (*e.g.*, Eracleous & Halpern 2003); it is difficult to understand how a larger disk could exhibit its brightest AGN-like emission at distances $\sim 1 \text{ kpc}$ from the SMBH. On the other hand, outflows of gas and dust are commonly invoked to explain asymmetric [O III] emission from narrow-line AGN (*e.g.*, Heckman et al. 1981). These asymmetries, however, typically take the form of broad, blue wings, not strong second peaks, and in this picture we would expect one emission component to be at rest at the host galaxy’s center, unlike what is observed here. There do exist, in a few nearby Seyferts, bipolar outflows that have spatial scales, bulk velocities, and emission-line ratios that could explain our observations (*e.g.*, Axon et al. 1998; Veilleux, Shopbell, & Miller 2001), but these systems are quite kinematically disturbed, with emission components whose velocity dispersions are comparable to their velocity separations. This contrasts strongly with the relatively narrow emission-line components in this object.

We thus regard a dual SMBH as the likeliest explanation for our observations. The identification is quite consistent with theoretical expectations and with previous observations. As discussed in the Introduction, dual SMBHs are expected to remain separated at $\gtrsim 1 \text{ kpc}$ for $\sim 100 \text{ Myr}$ after a galaxy merger and then rapidly form a parsec-scale binary. Indeed, like this one, the previously observed dual AGN in NGC 6240 (Komossa et al. 2003) has a separation $\sim 1 \text{ kpc}$. Unlike this one, that galaxy also shows strong signatures of recent merger activity, but since such signatures are quite subtle in dissipationless mergers, they will not be as obvious in our imaging. However, the identification of a dual AGN in this galaxy is not as secure as in NGC 6240, where *Chandra* can resolve two X-ray sources in the galaxies’ centers; the angular scale of interest here ($0''.17$) is simply too small to be resolved in our observations.

Nevertheless, assuming our interpretation is correct, it is possible to infer further information about the two SMBHs. First, they are clearly bound within the galaxy, since their peculiar velocities ($\sim 300 \text{ km s}^{-1}$) are much smaller than the escape velocity ($\sim 1000 \text{ km s}^{-1}$) implied by the host galaxy’s measured stellar mass. Second, our observations permit an es-

timate of the SMBH masses. Greene & Ho (2005) show that, in nearby AGN, the width of the [O III] emission lines is a reasonable proxy for the stellar velocity dispersion of the galaxy bulge, σ_* , provided that any asymmetric wings are removed. Our line-fitting procedure accounts for all obvious asymmetries, so we may use the measured linewidths to infer SMBH masses from the $M_{\text{BH}}-\sigma_*$ relation (*e.g.*, Greene & Ho 2006). This relation implies $M_{\text{BH}} \sim 5 \times 10^5 M_\odot$ for the blueward component and $M_{\text{BH}} \sim 5 \times 10^6 M_\odot$ for the redward one. By comparison, the relation between bulge mass and SMBH mass (*e.g.* Häring & Rix 2004) implies that this $M_* = 10^{11} M_\odot$ galaxy should harbor a BH of mass $\sim 10^8 M_\odot$, more than an order of magnitude larger than the total BH mass we infer. The discrepancy is only at the $\sim 2\sigma$ level, however, given the large scatter in the relations discussed here.

Simple considerations might lead one to expect that dual SMBHs reside in a relatively large fraction of galaxies: if a typical galaxy undergoes a major merger every few Gyr, and the resulting dual SMBH has a lifetime of ~ 100 Myr, then a few percent of all galaxies—say ~ 1000 of the ~ 40000 galaxies in DEEP2—should host such systems. The fact that we have found only one dual AGN in DEEP2 is not inconsistent with this estimate. First, it is not clear that *every* dual SMBH will exhibit AGN activity for its full lifetime, especially from both nuclei at once. Even if so, clean detection of double-peaked AGN emission lines is easiest if the bright, narrow [O III] emission lines fall in the DEEP2 wavelength range; this is true for only $\sim 30\%$ of the DEEP2 sample. Also, dual AGN that occur in late-type galaxies may have the bulk of their optical emission obscured by dust (*e.g.*, Zakamska et al. 2005), so we can expect objects with observational signatures like this one to occur mostly in early-type systems. These constitute only $\sim 15\%$ of the DEEP2 sample. Thus we would expect DEEP2 to have only a few dozen objects like the one studied here if all such objects are active. This dual AGN was discovered serendipitously; a comprehensive search of the DEEP2 catalog might find more.

We close by addressing the relatively weak emission bridging the two emission components in Figs. 1 and 2. As already mentioned, narrow [O III] lines in AGN spectra frequently exhibit asymmetric blue wings, probably from outflows (*e.g.*, Heckman et al. 1981). If such an outflow is present for the redward AGN here, it could explain the bridging emission. Given the unusual nature of this galaxy’s spectrum, however, this explanation is by no means certain. Infrared imaging and integral-field unit observations on an 8-meter class telescope with adaptive optics, or narrow-band imaging of the [O III] line from space, could help to further characterize this emission and the system as a whole.

We thank M. Boylan-Kolchin and E. Quataert and the anonymous referee for helpful comments. This work is based in part on observations made with the Spitzer Space Telescope, which is operated by the Jet Propulsion Laboratory, California Institute of Technology under

a contract with NASA. Support for this work was provided by NASA through an award issued by JPL/Caltech. The National Radio Astronomy Observatory is operated by Associated Universities, Inc. under a cooperative agreement with the National Science Foundation. Further relevant acknowledgments for this work are in Davis et al. (2006)

REFERENCES

- Axon, D. J., et al. 1998, *ApJ*, 496, L75
- Ballo, L., et al. 2004, *ApJ*, 600, 634
- Begelman, M. C., Blandford, R. D., & Rees, M. J. 1980, *Nature*, 287, 307
- Bruzual, G., & Charlot, S. 2003, *MNRAS*, 344, 1000
- Davis, M., et al. 2006, *ApJ*, in prep
- Elvis, M., et al. 1994, *ApJS*, 95, 1
- Eracleous, M., & Halpern, J. P. 2003, *ApJ*, 599, 886
- Faber, S. M., et al. 2005, *ApJ*, submitted (astro-ph/0506044)
- Gandhi, P., et al. 2001, (astro-ph/0106139)
- Greene, J. E., & Ho, L. C. 2005, *ApJ*, 627, 721
- Greene, J. E., & Ho, L. C. 2006, *ApJ*, 641, L21
- Guainazzi, M. et al. 2005, *A&A*, 429, 9
- Håring, N., & Rix, H.-W. 2004, *ApJ*, 604, L89
- Heckman, T. M., et al. 1981, *ApJ*, 247, 403
- Hudson, D. S., et al. 2006, *A&A*, in press (astro-ph/0603272)
- Ivezic, Z., Nenkova, M., & Elitzur, M. 1999, (astro-ph/9910475)
- Iverson, R. J., et al. 2006, *ApJ*, in prep.
- Junkkarinen, V., et al. 2001, *ApJ*, 549, L155
- Kauffman, G. 2003, *MNRAS*, p. 1055

- Kochanek, C. S., Falco, E. E. and Muñoz, J. A. 1999, *ApJ*, 510, 590
- Komossa, S., et al. 2003, *ApJ*, 582, L15
- Lotz, J., et al. 2006, *ApJ*, submitted (astro-ph/0602088)
- Maness, H. L., et al. 2004, *ApJ*, 602, 123
- Merritt, D., & Milosavljević, M. 2005, *Living Rev. Relativity*, 8, 8, (astro-ph/0410364)
- Milosavljević, M., et al. 2002, *MNRAS*, 331, L51
- Nandra, K., et al. 2006, *ApJ*, in prep.
- Peng, C. Y., et al. 2002, *AJ*, 124, 266
- Rodriguez, C., et al. 2006, *ApJ*, in press (astro-ph/0604042)
- Salim, S., et al. 2005, *ApJ*, 619, L39
- Sérsic, J. L. 1968. *Atlas de Galaxias Australes*, Córdoba: Obs. Astron., Univ. Nac. Córdoba
- van Dokkum, P., et al. 2005, *AJ*, 130, 2647
- Veilleux, S., Shopbell, P. L., & Miller, S. T. 2001, *AJ*, 121, 198
- Willmer, C. N. A., et al. 2005, *ApJ*, in press
- Yan, R., et al. 2006, *ApJ*, in press. (astro-ph/0512446)
- Zakamska, N. L., et al. 2005, *AJ*, 129, 1212

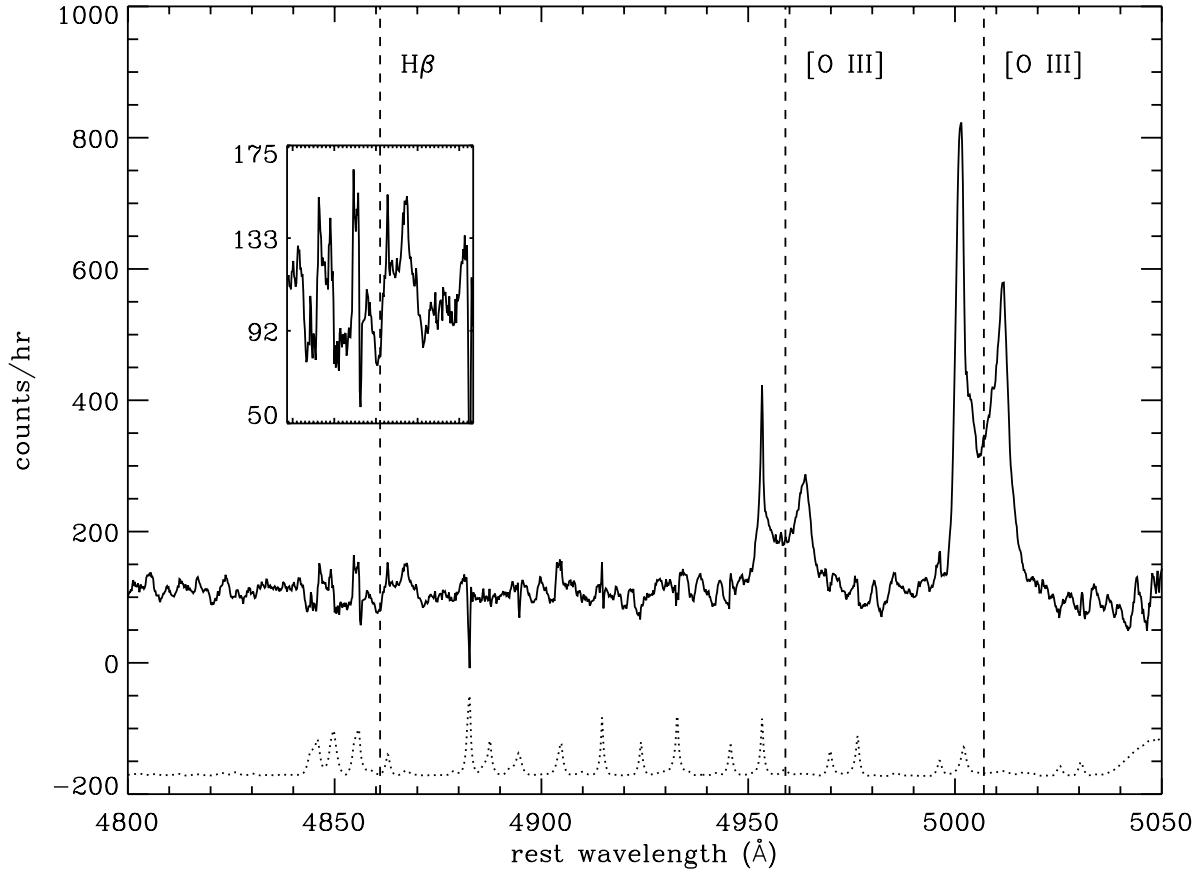


Fig. 1.— A portion of the one-dimensional DEIMOS spectrum of the dual-AGN host galaxy (solid line). Night-sky emission has been subtracted, and the spectrum has been weighted by its inverse variance and smoothed with a ten-pixel-wide top-hat kernel. The dotted line shows the Poisson uncertainty in the smoothed spectrum, scaled up by a factor of three and offset for clarity. The wavelength scale has been shifted to the host galaxy’s rest frame (see text); dashed vertical lines show the expected wavelengths of [O III] and H β emission. Each [O III] line has two clear emission components separated by 630 km s $^{-1}$ in velocity. For clarity, the H β emission is shown on a magnified vertical scale in the inset; it is affected by noise from a night sky line.

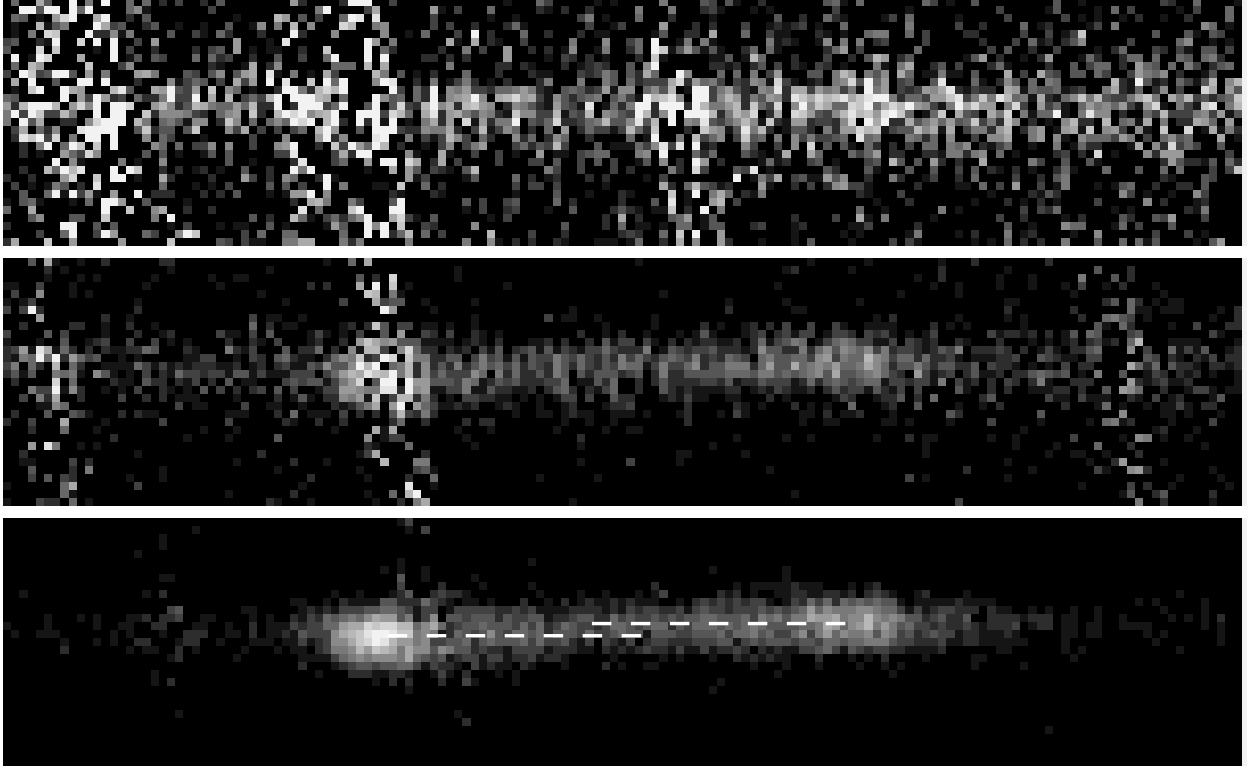


Fig. 2.— Two-dimensional spectral emission on the DEIMOS detector in the vicinity of the emission lines seen in Fig. 1, after sky subtraction. In each panel, wavelength increases to the right, and spatial position along the slit (oriented at position angle 41°) is represented in the vertical direction. From top to bottom, the lines shown are $H\beta$ (partially obscured by night-sky noise), $[O\ III]\lambda 4959$, and $[O\ III]\lambda 5007$. Horizontal dashed lines in the bottom panel show the spatial centroids of the two emission line components, which are offset from each other by 1.5 DEIMOS pixels, or $0''.17$. This corresponds to a projected separation of 1.2 kpc.

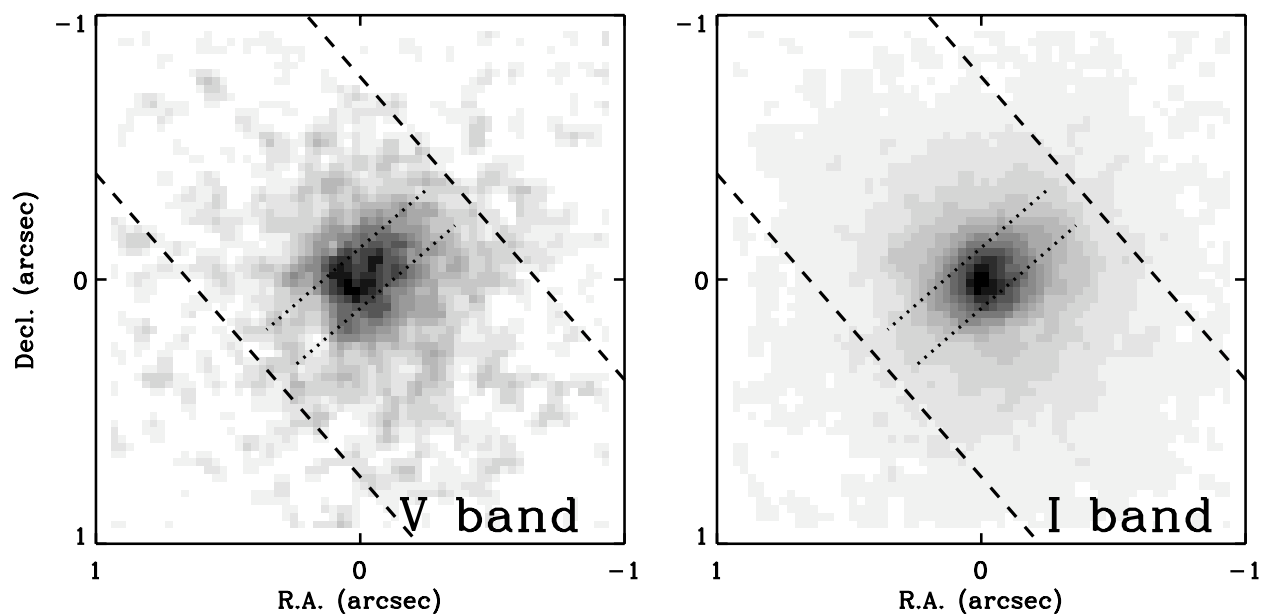


Fig. 3.— *HST*/ACS images of the host galaxy in the F606W and F814W (*V* and *I*) bands. Both images are shown with a logarithmic intensity scale and have been smoothed by a Gaussian kernel with a 1.5-pixel FWHM. The galaxy appears to be spheroidal, with a roughly circular profile, but both images show subtle asymmetries, possibly indicating disturbed structure. Also shown are the edges of the DEEP2 DEIMOS slit (dashed lines; approximately 50% of the full slit length is shown) and the positions along the slit of the two emission-line components in Fig. 2 (dotted lines).

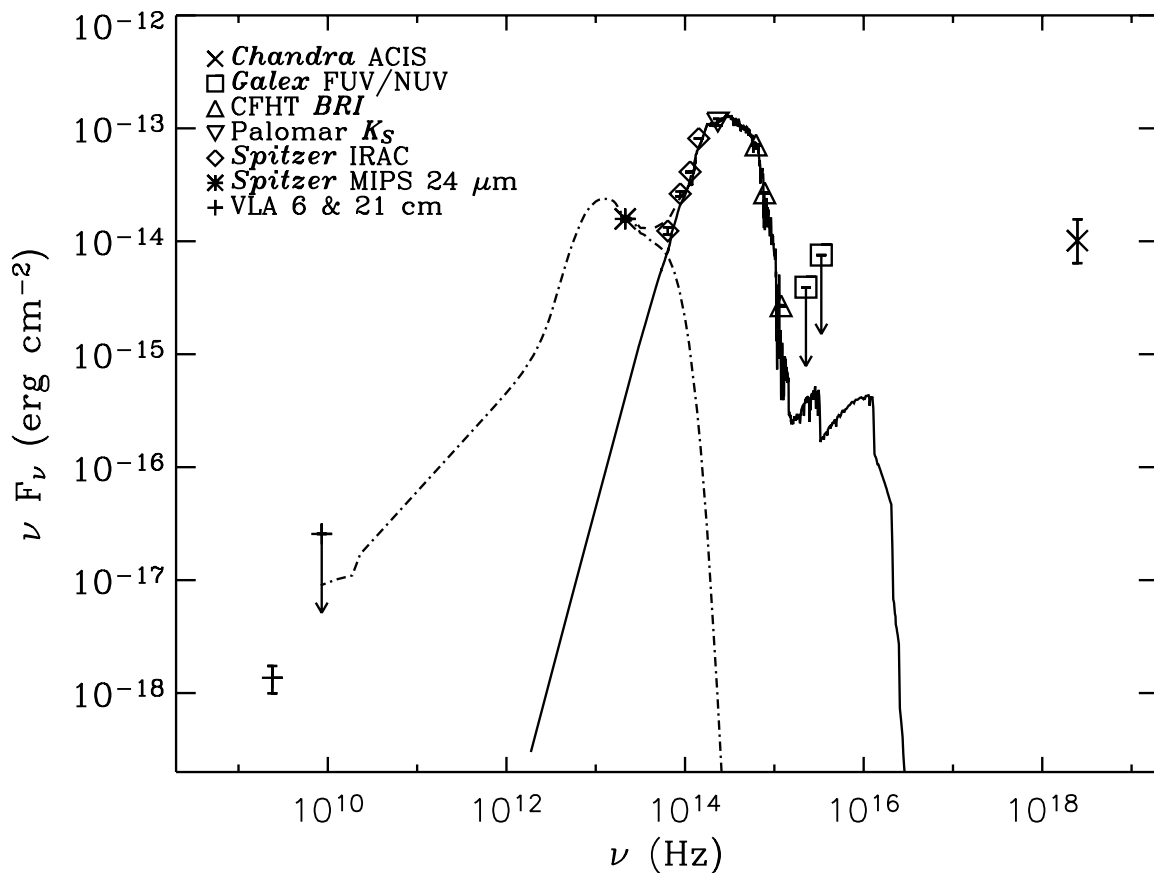


Fig. 4.— Spectral energy distribution of the dual AGN and host galaxy, from radio to X-ray. Data points show fluxes (or upper limits) measured by various instruments, as noted in the legend. All frequencies have been shifted to the host galaxy’s rest frame. Also shown are a template spectrum for an early-type galaxy (see text) normalized to the K-band flux (solid line) and a simple model for infrared emission from a dust-obscured AGN normalized to the MIPS 24 μm flux (dot-dashed line). The dashed line (visible at center) shows the sum of the dust and stellar models.